Available online at www.sciencedirect.com
SCIENCE DIRECT®
Spectrochimica Acta Part A 60 (2004) 3431–3436
SPECTROCHIMICA ACTA PART A
www.elsevier.com/locate/saa

Application of antimonide diode lasers in photoacoustic spectroscopy

Stéphane Schilt[a,*], Aurore Vicet[b], Ralph Werner[c], Mario Mattiello[a], Luc Thévenaz[a], Abdelmajid Salhi[b], Yves Rouillard[b], Johannes Koeth[c]

[a] *Laboratory of Nanophotonics and Metrology (NAM), Swiss Federal Institute of Technology (EPFL), CH-1015 Lausanne, Switzerland*
[b] *Centre d'Electronique et de Microoptoélectronique de Montpellier (CEM2 UMR CNRS 5507), Université Montpellier II, F-34095 Montpellier Cedex 05, France*
[c] *Nanoplus Nanosystems and Technology GmbH, Oberer Kirschberg 4, D-97218 Gerbrunn, Germany*

Received 1 October 2003; accepted 12 November 2003

Abstract

First investigations of photoacoustic (PA) spectroscopy (PAS) of methane using an antimonide semiconductor laser are reported. The laser fabrication is made in two steps. The structure is firstly grown by molecular beam epitaxy, then a metallic distributed-feedback (DFB) grating is processed. The laser operates at 2371.6 nm in continuous wave and at room temperature. It demonstrates single-mode emission with typical tuning coefficients of 0.04 nm mA^{-1} and 0.2 nm K^{-1}. PA detection of methane was performed by coupling this laser into a radial PA cell. A detection limit of 20 ppm has been achieved in a preliminary configuration that was not optimised for the laser characteristics.

Keywords: Photoacoustic spectroscopy; Antimonide; Semiconductor lasers; DFB; Trace gas monitoring

1. Introduction

Trace gas monitoring by optical absorption spectroscopic techniques with laser diodes provides a highly sensitive and selective detection with a short response time. Among possible methods, photoacoustic (PA) spectroscopy (PAS) is of great interest. This well-established technique consists in the generation of an acoustic wave in a sample excited by a modulated laser beam, and in the detection of this sound wave with a sensitive microphone.

PAS was primarily developed using high power gas lasers (such as CO or CO_2 lasers) in order to reach extreme detection limits, usually in the parts-per-billion (ppb) range. However, many applications require a lower sensitivity, typically in the parts-per-million (ppm) or sub-ppm levels, and semiconductor distributed-feedback (DFB) lasers are of great interest in this case. They are very compact and robust sources in comparison to large size gas lasers and have a much longer lifetime. They are also continuously tunable, enabling a precise adjustment of the laser wavelength on the centre of an absorption line of the substance to be detected, whereas the discrete line-by-line tunability of gas lasers requires an accidental coincidence between an absorption line of the species and an emission line of the laser. The main disadvantage of semiconductor lasers is the strongly reduced optical power (typically in the 1–10 mW range) in comparison to gas lasers (several watts). In conjunction with the usually smaller absorption line strengths in the near-infrared than in the 10 μm emission range of CO_2 lasers, the sensitivity of semiconductor laser-based photoacoustic systems is 2–3-orders of magnitude worse than for CO_2 laser-based configurations. However, sufficient sensitivities for many applications can be obtained in PA spectrometers properly designed to take into account the characteristics of these lasers. Resonant configurations with high enhancement factors or multipass PA cells [1,2] offer thus an attractive potential.

Different types of semiconductor lasers have been used in trace gas monitoring applications. The more commonly used are near-infrared InP-based lasers primarily developed for optical telecommunications. These technologically matured devices of high reliability emit in the 1.1–2.0 μm range, where overtone absorption bands of many molecules are

* Corresponding author. Tel.: +41-21-693-3969; fax: +41-21-693-2614.
E-mail addresses: stephane.schilt@epfl.ch (S. Schilt), a.vicet@univ-montp2.fr (A. Vicet), ralph.werner@nanoplus.com (R. Werner).

1386-1425/$ – see front matter © 2004 Elsevier B.V. All rights reserved.
doi:10.1016/j.saa.2003.11.045

present. Lead salt and quantum cascade lasers (QCL) give access to the strong fundamental absorption bands of many atmospheric species in the mid-infrared (5–20 μm). The intermediate 2–2.5 μm range is also of great interest, as it enables to enhance the detection sensitivity of many species in comparison to the near-infrared, while keeping the main advantages of this spectral range. For example, lasers made of antimonide-based materials have been demonstrated in this spectral range with continuous wave and room temperature operation. Photodiodes also operate at room temperature with good sensitivities in comparison to mid-infrared detectors. Finally, standard glass optical components, such as lenses or windows, remain usable with reasonable optical losses. The 2–2.5 μm range is located in an atmospheric transmission window, where absorption by water vapour or carbon dioxide is weak, which makes this region very attractive for atmospheric and industrial applications. Many species of environmental interest present strong absorption lines in this window (CH_4, NH_3, HF, CO, ...) and can be efficiently detected. For example, the strongest lines in the $\nu_1 + \nu_4$ band of methane at 2.37 μm are twice greater than in the $2\nu_3$ band at 1.65 μm, whereas an enhancement factor of 225 is expected for CO when going from 1.57 μm (4ν band) to 2.33 μm (3ν band).

In spite of these attractive properties, few groups are currently involved in laser developments and spectroscopic applications in this spectral range. To our knowledge, PA measurements made with room-temperature antimonide lasers have never been published and the only reported results have been obtained using a laser cooled at cryogenic temperature [3]. We present in this paper first investigations of PAS using a room-temperature antimonide DFB laser diode. The laser structures were grown at CEM2 in Montpellier University (France), then a lateral DFB grating was processed in Nanoplus (Germany). PA experiments were made in EPFL (Switzerland), using a PA cell previously designed for CO_2 laser-based sensing. The cell has not been optimised for the characteristics of the antimonide laser yet. Methane detection has been performed by coupling this PA cell to a first processed antimonide DFB laser, emitting at 2.37 μm.

2. Antimonide DFB laser diodes

2.1. Laser fabrication

CEM2 of Montpellier University is studying and fabricating antimonide-based laser diodes by molecular beam epitaxy (MBE) on GaSb substrates. The laboratory develops Fabry–Perot interband edge emitting laser, quantum cascade lasers and vertical (external) cavity surface emitting lasers (V(E)CSELs). Fabry–Perot lasers are typically working continuous wave at room temperature. Under particular conditions of injected current and temperature, they show alternating regions of single frequency and multimode emission. The use of a DFB technology enables to stabilise the emission wavelength on a single mode of the cavity, which lets the device remain single frequency.

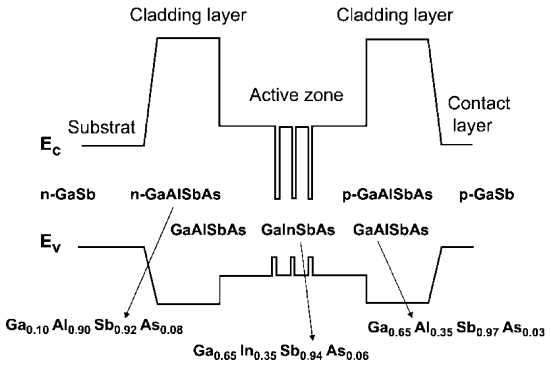

Fig. 1. Typical profile of the conduction and valence bands in the InGaAsSb/AlGaAsSb-based quantum wells lasers.

Collaboration between CEM2 and Nanoplus was born with the European project gas laser analysis by infrared spectroscopy (GLADIS). CEM2 supplied epitaxied wafers to Nanoplus, which processed them into DFB devices. The structure was grown in a Varian GenII MBE system equipped with Al, Ga, In, Be (for p-type doping), Te (for n-type doping) cells and As and Sb cracker cells generating As_2 and Sb_2 molecules. The growth temperature was fixed at 480 °C. The layers were grown in the following order (see Fig. 1): a 75 nm-thick n-type GaSb buffer, a 170 nm-thick n-layer graded from $Al_{0.10}Ga_{0.90}As_{0.03}Sb_{0.97}$ to $Al_{0.90}Ga_{0.10}As_{0.08}Sb_{0.92}$, a 1.5 μm-thick $Al_{0.90}Ga_{0.10}As_{0.08}Sb_{0.92}$ n-type (2×10^{18} cm^{-3}, Te) cladding layer, an undoped active zone consisting of three 10 nm-thick 1.9% compressively strained quantum wells of $Ga_{0.65}In_{0.35}As_{0.06}Sb_{0.94}$ separated by two $Al_{0.35}Ga_{0.65}As_{0.03}Sb_{0.97}$ electronic barriers giving a type I band alignment [4] and enclosed between 355 nm-thick $Al_{0.35}Ga_{0.65}As_{0.03}Sb_{0.97}$ spacers, a 1.5 μm-thick p-type $Al_{0.90}Ga_{0.10}As_{0.08}Sb_{0.92}$ (5×10^{18} cm^{-3}, Be) cladding layer, a 170 nm-thick p-layer graded from $Al_{0.90}Ga_{0.10}As_{0.08}Sb_{0.92}$ to $Al_{0.10}Ga_{0.90}As_{0.03}Sb_{0.97}$, and finally a 0.5 μm p^+-GaSb cap layer. The doping level of the first 0.2 μm of the upper cladding near the active zone was decreased to 5×10^{17} cm^{-3} in order to reduce the free carriers absorption.

The wafer was then processed by Nanoplus. They defined a narrow ridge waveguide and processed a chromium grating along the ridge by electron beam lithography, to select one mode according to the Bragg equation. The grating period was around 350 nm. The devices are epi side up mounted on standard TO mounts.

2.2. Laser characterisation

The DFB laser diodes showed typically 40 mA of threshold current at room temperature and output powers of 6–8 mW at 250 mA (see Fig. 2). A good temperature stability was achieved, with a characteristic temperature T_0 of 120 K (see Fig. 2).

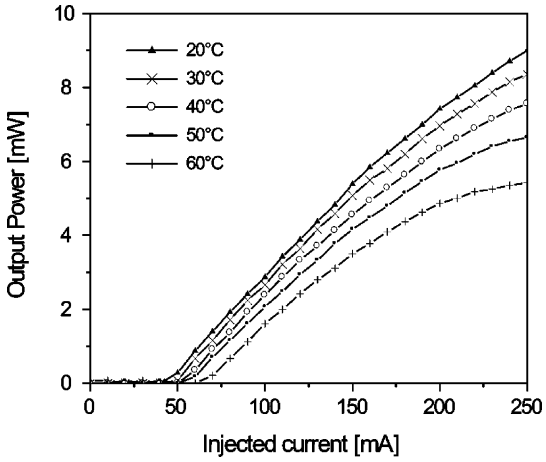

Fig. 2. *L–I* curves of the DFB laser diode, in continuous wave regime. The evolution of threshold current with temperature gives a characteristic temperature of 120 K.

The tuning properties are mainly explained by the effect of the temperature and are about 0.04 nm mA^{-1} for current tuning at fixed temperature and 0.2 nm K^{-1} for temperature tuning at a fixed injected current. These high tuning values are explained by the large value of the thermal resistance $R_{th} = 130\,K\,W^{-1}$. Those values make the device well adapted to gas detection, even at atmospheric pressure where the absorption lines are as large as a few gigahertz [5].

Fig. 3 shows the evolution of the normalised emission spectra of the device and the corresponding values of the side mode suppression ratio (SMSR), measured using a grating monochromator. A nice single-mode evolution with a SMSR superior to 30 dB is observed.

The spatial distribution of the laser emission was also measured using a small surface (diameter 250 μm) extended InGaAsP photodetector mounted on a motorised translation stage directly in front of the laser, i.e. with no collecting optics. The detected power was measured in both directions as

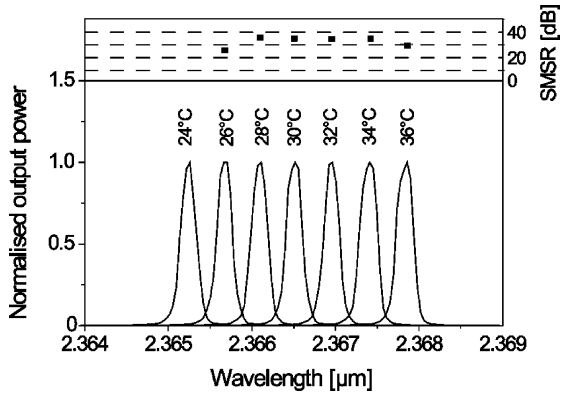

Fig. 3. Emission spectra for a continuous injected current $I = 120$ mA at different temperatures. A high side mode suppression ratio and a good stability of the emitted wavelength have been achieved using the DFB process.

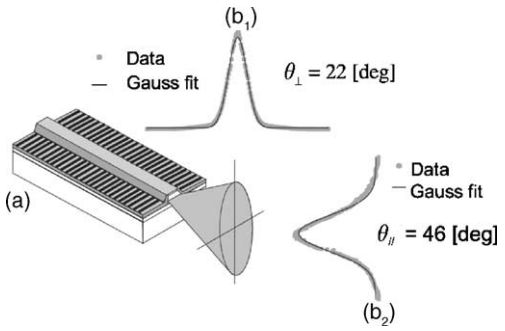

Fig. 4. Divergence of the antimonide laser emission. (a) Schematic representation and (b) spatial distributions of the laser beam measured in the horizontal (b_1) and vertical (b_2) directions. The grey points are experimental data and the black lines are the result of a fit.

a function of the detector position, which gave the horizontal and vertical profiles of the laser beam. The measured profiles were then fitted in order to determine the beam waists in both directions (half width at $1/e^2$). A Gaussian curve fitted very well the experimental points in the horizontal direction. However, the measured vertical profiles were systematically slightly asymmetric, so that the fit by a Gaussian distribution was well adjusted on the experimental points only on one side of the profile, whereas a fit by a Lorentzian distribution was better on the other side. The beam diameter was thus defined as the average of the values given by the Gaussian and Lorentzian fits. The divergence angles of the laser emission were determined by measuring the beam waists at different distances from the laser. Divergences of 22° horizontally and 46° vertically (half angle at $1/e^2$) were obtained. Fig. 4 illustrates an example of the beam distributions measured in both directions. The laser divergence is also shown schematically. It appears to be much higher in the vertical direction than in the horizontal, due to the dimensions (0.8 μm × 2 μm) of the optical waveguide. Due to this high divergence, the laser emission is poorly collected by a collimating optics, resulting in large optical losses.

3. Photoacoustic spectroscopy

3.1. Theoretical background

As other traditional spectroscopic methods, PAS is based on molecular absorption of a laser beam. However, instead of measuring the quantity of light transmitted through the sample, as in conventional techniques, the fraction of absorbed light is directly determined. A modulated laser beam of suitable wavelength is absorbed by the gas molecules. The non-radiative relaxation of the excited molecules produces a temperature variation and hence, a pressure modulation (i.e. a sound wave), that is detected using a microphone. In addition to its simplicity and sensitivity, PAS is a zero-background technique, as no signal is produced when the molecules of interest are absent.

The theory of the generation and detection of the PA signal in a cylindrical cell has been presented in detail by several authors ([6–9]). In the case of small absorption, the PA signal S_{PA} is directly proportional to the laser power P_0 and to the molecular absorption coefficient α:

$$S_{PA} = C_{cell}\alpha P_0, \quad (1)$$

where C_{cell} is a scaling factor depending on the PA cell geometry, on the modulation frequency and on some physical parameters of the gas. This coefficient, called the cell constant, is generally derived experimentally from measurements performed in well-controlled conditions, with a gas of known absorption and with a certified concentration.

Resonant PA configurations enable an enhancement of the PA signal, thanks to resonance effect occurring in the cell, which acts as an acoustic resonator. When the laser modulation frequency is adjusted on a resonance frequency of the cavity, a standing wave occurs in the cell. The cell constant is given in this case by

$$C_{cell} = \frac{Q_j}{\omega_j}\frac{(\gamma-1)I_j L_c}{V_c}p_j(r_M, \omega_j), \quad (2)$$

where $\gamma = C_p/C_v$ is the ratio of the specific heat at constant pressure and constant volume, Q_j is the quality factor of the resonance, ω_j the angular resonance frequency, V_c the cell volume, L_c the cell length, $p_j(r_M, \omega_j)$ the value of the normalised acoustic mode at the position r_M of the microphone and I_j is the overlap integral between the laser beam and the acoustic mode. To achieve a good sensitivity, the PA cell must be optimised in order to reach a high cell constant.

3.2. Experimental

Our experimental set-up is made of an antimonide DFB laser, a resonant PA cell and a powermetre for PA signal normalisation. This apparatus is shown schematically in Fig. 5. The laser is mounted on a window-less TO-5.6 mm package and is temperature-stabilised using a commercial TE-cooled laser mount (Thorlabs TCLDM9). The laser temperature is tuned to reach the proper emission wavelength and the injection current is modulated in order to excite an acoustic resonance of the PA cell. The modulation frequency is continuously and automatically adjusted on the corresponding resonance frequency. The strongly diverging laser emission

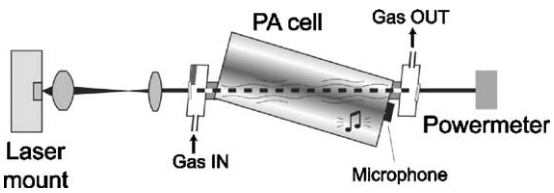

Fig. 5. Schematic experimental set-up of PAS using an antimonide DFB laser, a radial PA measurement cell and an optical powermetre. The amplitude of the first radial mode is shown in greyscale with the pressure nodes in white. The laser beam enters and leaves the resonator at the nodes of the radial mode.

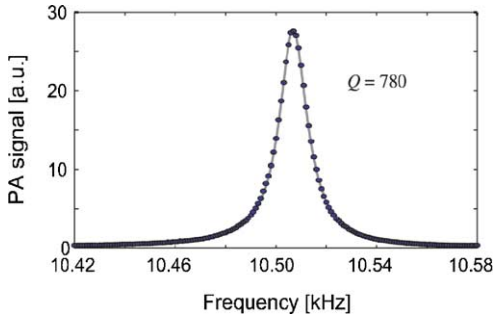

Fig. 6. First radial acoustic resonance of our PA cell at 10.5 kHz. Circles are experimental points and the curve is the result of a fit by a Lorentzian distribution. The quality factor $Q = 780$.

is collected using a short focal lens of numerical aperture NA = 0.5 and is then collimated using a second lens (20 mm focal length).

The PA cell is made of central cylindrical resonator and two buffer volumes acting as acoustic filters. The acoustic resonator is operated in its first radial mode at $f = 10.5$ kHz, as shown in Fig. 6. The acoustic signal is detected with an electret microphone located on the cell axis, i.e. at the position of the maximum acoustic amplitude, and is measured with a lock-in amplifier. The radial resonance shows a high quality factor, $Q = 780$. This PA cell was in fact optimised to be used with a collimated high power CO_2 laser. The selected configuration is well suited for high power lasers, as it minimises the coupling of the window noise into the resonator [10]. However, it is not the best configuration for the characteristics of the antimonide laser used in these experiments. First of all, radial configurations are not the most sensitive (in comparison to longitudinal modes for example), when window noise is not an issue, which is always the case with low power semiconductor lasers. Furthermore, the coupling of the laser emission into the PA cell was poorly efficient due to the high divergence of the laser emission and to the inappropriate coating on the cell windows. However, PA detection of methane has been accomplished using this experimental set-up and has shown promising results.

3.3. Results and discussion

The PA spectrum of methane has been measured by tuning the laser wavelength (temperature tuning) in order to select the strongest absorption line. The measured spectrum is shown in Fig. 7 and is compared with the absorption spectrum calculated from the HITRAN database [11]. A good qualitative agreement is obtained, but the measured spectrum has a slightly reduced spectral resolution. This is due to a broadening of the laser linewidth induced by the current modulation. The laser wavelength probably shifts during the current pulses due to heating. This effect is important in this laser as the temperature stabilisation (TE cooler) is not integrated directly in the laser housing, as it is usually the case in packaged laser diodes, but was located outside. The

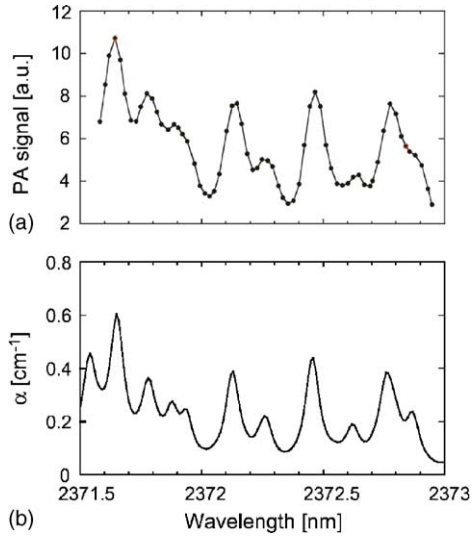

Fig. 7. (a) PA spectrum of methane measured with our experimental set-up; the laser wavelength is tuned by changing the laser temperature. (b) Absorption spectrum of methane calculated from HITRAN database.

thermal dissipation is therefore less efficient with the whole TO mount placed on the TE-cooled laser mount. This effect is still increased as the laser is mounted junction up. The measured photoacoustic spectrum is thus the convolution between the true absorption spectrum and the laser lineshape. The experimental spectrum shown in Fig. 7 has been obtained with laser operating current and modulation depth optimised to achieve a good resolution. The corresponding laser power was reduced by a factor 2 in comparison to the value that could be reached if the full scale of current could be used. Worse spectra were observed when larger modulation amplitudes or higher average currents were used.

The strongest absorption line at 2371.6 nm was selected for methane detection. In order to evaluate the performances of our system, methane concentration was changed by dilution in pure nitrogen using mass flow controllers. The response of the PA system for various methane concentrations is shown in Fig. 8. For each concentration step, the average value and the deviation of the PA signal were measured. The

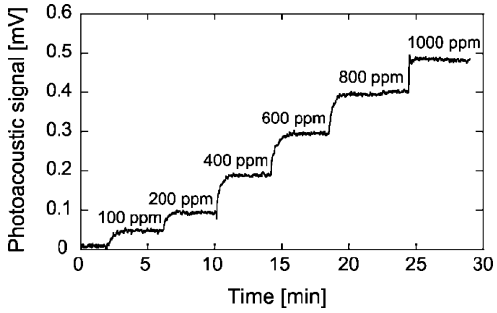

Fig. 8. Response of the PA signal for varying methane concentrations. The laser emission is centred on the CH_4 absorption line at 2371.6 nm. The methane concentration was changed by dilution in pure nitrogen using mass flow controllers.

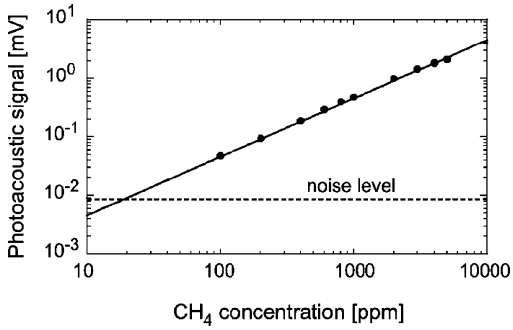

Fig. 9. Variation of the PA signal at 2371.6 nm as a function of the methane concentration. The background level is also indicated, corresponding to a CH_4 detection limit of 20 ppm.

PA signal responds with an excellent linearity to the varying methane concentration, as shown in Fig. 9. The background (noise) level measured by flowing pure nitrogen into the cell was lower than 10 μV. With a typical microphone sensitivity of 10 mV Pa^{-1} and taking into account the gain ($G = 200$) of the preamplifier, it corresponds to a pressure amplitude of 5 μPa. This noise level corresponds mainly to ambient acoustic noise and microphone intrinsic noise. No windows noise or flow noise has been observed, even for flow rates as high as 1000 ml min^{-1}. From this noise level, a detection limit of 20 ppm of methane is determined in the current configuration.

Taking into account the low optical power injected in the PA cell (typically 0.3 mW), the obtained sensitivity is comparable to results previously reported in the 1.65 μm range using standard telecommunication DFB lasers and longitudinal acoustic resonators [12–14], but slightly lower than values reached using differential Helmholtz resonators [15,16]. These results are however far from the best reported sensitivity (close to 1 ppb) for PA methane detection [17], achieved in the 3.3 μm region, where the CH_4 absorption is more than one-order of magnitude higher than in the 1.65 or 2.37 μm ranges, and with a 200 times higher optical power delivered by an optical parametric oscillator. These first investigations with antimonide lasers are therefore very promising and progresses in several domains are expected to improve the current detection limit to reach a sub-ppm level in a near future. Improvements are expected to result from both laser and PA cell. For the laser, the problem of linewidth broadening in presence of high modulation depths needs to be reduced in order to enable the use of larger modulation indexes. An enhancement of the PA signal of a factor 2 is thus expected. A new PA cell design to be used with antimonide lasers is also under study. This new design aims at optimising the cell geometry to take into account the laser properties. The objective is to increase the cell constant on one hand and to improve the coupling of the laser emission into the cell on the other hand. In the present configuration, the light coupling efficiency is as low as 20%. An enhancement of the PA signal of one-order of magnitude can be reasonably expected from all these improvements.

4. Conclusions

Antimonide-based DFB lasers emitting in continuous wave at room temperature have been demonstrated. The lasers are manufactured in two steps. The laser structure is first grown by MBE, then a lateral metallic DFB grating is processed. Single-mode emission has been obtained in the 2.37 μm range with a SMSR higher than 30 dB and typical output powers of several mW. The tuning properties of these lasers make them good candidates for trace gas monitoring applications and first investigations in PAS have been performed. The laser beam was coupled into a resonant PA cell and the injection current was modulated at the frequency of the first radial resonance of the acoustic resonator. Methane was detected in this experimental set-up at of wavelength of 2371.6 nm. The comparison between HITRAN simulation and gas measurements has shown a broadening of the absorption lines explained by a broadening of the laser linewidth under pulsed injection. A detection limit of 20 ppm CH_4 has been reached, even with the low optical power injected into the PA cell. This sensitivity is comparable to some results previously reported in the 1.65 μm range using standard telecommunications DFB lasers and absorption lines of similar intensities. The low optical power injected into our PA cell is mainly due to the poor collecting efficiency of the highly diverging laser emission. Furthermore, the PA cell used in these experiments was not optimised for the laser emission properties. A new configuration taking better into account these characteristics is currently under development. It should enable to reach a higher cell constant and a better light coupling into the cell. An improvement of one-order of magnitude in the CH_4 detection limit is thus expected with this new configuration.

Acknowledgements

This work is partly supported by the European Community through the GLADIS contract (IST-2001-35178). The authors from Montpellier are also grateful to the Languedoc-Roussillon Region for its support. Authors from EPFL are grateful to Omnisens SA for supporting this research.

References

[1] M. Nägele, D. Hofstetter, J. Faist, M.W. Sigrist, Anal. Sci. 17 (2001) 497–499.
[2] Ch. Hornberger, M. König, S.B. Rai, W. Demtröder, Chem. Phys. 190 (1995) 171–177.
[3] P. Kania, S. Civis, Spectrochim. Acta A 59 (2003) 3063–3074.
[4] A. Yarekha, G. Glastre, A. Perona, Y. Rouillard, F. Genty, E.M. Skouri, G. Boissier, P. Grech, A. Joullié, C. Alibert, A.N. Baranov, Electron. Lett. 36 (6) (2000) 537–539.
[5] A. Vicet, D.A. Yarekha, A. Perona, Y. Rouillard, S. Gaillard, A.N. Baranov, Spectrochim. Acta A 58 (11) (2002) 2405–2412.
[6] L.B. Kreuzer, in: Y.-H. Pao (Ed.), Optoacoustic Spectroscopy and Detection, Academic Press, New York, 1977, pp. 1–25 (Chapter 1).
[7] A. Miklos, P. Hess, Z. Bozoki, Rev. Sci. Instrum. 72 (4) (2001) 1937–1955.
[8] S. Schilt, Détection de traces de gaz à l'aide de lasers à semi-conducteurs, Ph.D. dissertation no. 2525, Swiss Federal Institute of Technology, Lausanne, 2002.
[9] P.L. Meyer, M.W. Sigrist, Rev. Sci. Instrum. 61 (7) (1990) 1779–1807.
[10] R. Gerlach, N. M Amer, Appl. Phys. 23 (1980) 319–326.
[11] L.S. Rothman, et al., J. Quant. Spectrosc. Radiat. Transfer 60 (1998) 665–710.
[12] S. Schäfer, M. Mashni, J. Sneider, A. Miklós, P. Hess, H. Pitz, K.-U. Pleban, V. Ebert, Appl. Phys. B 66 (1998) 511–516.
[13] A. Boschetti, D. Bassi, E. Iacob, S. Ionnatta, L. Ricci, M. Scotoni, Appl. Phys. B 74 (2002) 273–278.
[14] G.-C. Liang, H.-H. Liu, A.H. Kung, A. Mohacsi, A. Miklos, P. Hess, J. Phys. Chem A 104 (2000) 10179–10183.
[15] V.A. Kapitanov, V. Zéninari, B. Parvitte, D. Courtois, Yu.N. Ponomarev, Spectrochim. Acta A 58 (2002) 2397–2404.
[16] V. Zéninari, B. Parvitte, D. Courtois, V.A. Kapitanov, Yu.N. Ponomarev, Infrared Phys. Technol. 44 (2003) 253–261.
[17] A. Miklós, C.-H. Lim, W.-W. Hsiang, G.-C. Liang, A.H. Kung, A. Schmohl, P. Hess, Appl. Optics 41 (15) (2002) 2985–2993.